Impact of Antenna Downtilt on Cooperative Uplink Detection in a Large Scale Field Trial

Michael Grieger, Gerhard Fettweis
Technische Universität Dresden,
Vodafone Chair Mobile Communications Systems,
Email: {michael.grieger, fettweis}@ifn.et.tu-dresden.de

***Abstract*—The spectral efficiency of today's cellular networks that feature small inter-site distance and high spectral reuse is limited by inter-cell interference. An effective means to cope with the signal radiation across cell boundaries in the cellular uplink is joint detection of multiple users at cooperative base stations (BSs), a concept known as network MIMO or coordinated multi-point (CoMP). However, it is well known that the cluster size of cooperating base stations is limited in a real system due to backhaul, latency and signaling constraints. Thus, cooperation of base station needs to be applied jointly with other methods for inter cell interference reduction. An important lever is the usage of antenna downtilt to control the direction of the vertical antenna pattern and, therefore, the distance of signal propagation. In this work, we investigate the effect of the antenna downtilt on the performance of cooperative uplink detection in a large scale field trial and show the importance of downtilt optimization for cooperative systems.**

I. Introduction

The spectral efficiency of today's cellular systems is limited by inter-cell interference. Especially, data rates for mobile users that are located at cell edges are drastically reduced by this effect resulting in a lack of fairness that is identified as one of the major deficiencies of LTE Release 8. Some of the currently most promising proposals, for an improved system setup consider the use of CoMP techniques for the uplink and downlink. Field trial results (e.g. [1], [2]) of these techniques verify large improvements in spectral efficiency and fairness that were previously predicted by theory and simulation studies (e.g. [3], [4]).

In practical systems, however, the number of BSs that can cooperate for the detection of a certain set of user equipments (UEs) is limited because of the required pilot signal overhead, as well as backhaul and latency constraints [5]. The particular set of BSs that cooperate to detect a certain number of users is referred to as a cooperation cluster. The vast number of interferers outside the cluster add to an interference floor that limits the achievable signal-to-outer-cluster-interference ratio (SOCIR) and, therefore, the system performance. Thus, cooperation of BSs needs to be applied jointly with other methods for inter cell interference reduction. An outstanding lever, that is successfully exploited in the roll out of previous cellular standards, is to adapt the antenna radiation pattern with the aim to reduce inter-cell interference by taking the deployment and physical layer characteristics into account. For this purpose modern BS antennas typically provide mechanical and electrical means for a modification of their downtilt (the elevation angle corresponding to the highest directional antenna gain). The impact of the downtilt on system performance is well studied for WCDMA [6], but possible cooperation of BSs certainly has an impact on optimal downtilt settings as addressed and investigated by simulations in [7]. In this work, we investigate the impact of antenna downtilt on a CoMP uplink in a large scale field trial where two UEs are detected at clusters of up to three BSs. For this setting, we show that while achievable rates are only marginally effected by the downtilt, outer cluster interference can be substantially reduced by increasing the antenna downtilt, i.e. reducing the distance where the main antenna beam first hits the ground.

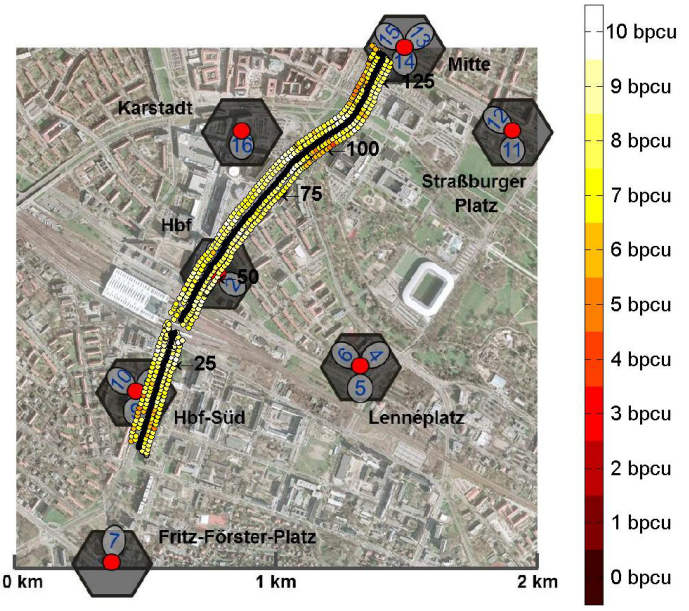

Fig. 1. Field trial setup and measurement trajectory (black curve). The other curves indicate the sum rate achieved by joint detection of 2 UEs at two cooperating BSs with $N_{\text{bs}} = 2$ antennas each. Each curve is showing the result for a particular antenna downtilt (at each BS of $\Phi_{\text{t}} = 0°, 6°, 9°, 12°$ from the left to the right. Map data © Sandstein Neue Medien GmbH (http://stadtplan.dresden.de)

In the sequel, the measurement setup is described in Section II, after which details of the signal processing architecture are provided in Section III. The field trial results are presented in Section IV. The paper is concluded in Section V.

TABLE I
TRANSMISSION PARAMETERS.

BS distance	350 - 600 m
BS antenna height	30 - 55 m
UE distance	about 5 m
UE antenna height	1.5 m
Number of antennas per BS	$N_{\text{bs}} = 1$
Carrier frequency	2.53 GHz
System bandwidth	20 MHz
Sampling frequency	$r_{\text{s}} = 30.72$ MHz
Num. physical resource blocks (PRBs)	30
Sub-carriers per PRB	12
UE transmit power	18 dBm
Quantization resolution	12 bit per real sample (bprs)

TABLE II
MODULATION SCHEMES AND CODE RATES USED FOR TRANSMISSION.

MCS#	Mod. scheme	Code rate	Peak rate (Mbps)	Bit per channel use (bpcu)
1	4QAM	3/16	1.3	0.375
2	4QAM	1/2	3.46	1.0
3	16QAM	2/5	5.62	1.6
4	16QAM	4/7	7.99	2.29
5	16QAM	3/4	10.6	3.0
6	16QAM	6/7	12.3	3.43
7	64QAM	3/4	16.3	4.5
8	64QAM	7/8	18.72	5.25

II. FIELD TRIAL SETUP

The field trial setup consists of 16 BSs deployed at 7 sites in downtown Dresden, as shown in Figure 1, and two UEs that are assembled on a measurement bus. Time and frequency synchronization of BSs, which is required for joint detection, is done through GPS fed reference normals. Each BS is equipped with a two element, cross-polarized KATHREIN 80010541 antenna which has 58° horizontal and 6.1° vertical half power beam width. We refer the reader to [8] for an illustration of the radiation pattern of this antenna. The UEs share the same time and frequency resources. Employing one dipole antenna, they transmit using orthogonal frequency division multiplexing (OFDM) while they are moved on a measurement trajectory as depicted in Figure 1. All UEs are configured to use the same modulation and coding scheme (MCS), whereas the MCS is switched in a fast sequence according to Table II. Thus, within the channel coherence time, different transmission rates can be tested. In order to investigate the impact of the BS antenna downtilt the measurement route is repeated for four different downtilts between 0° - 12°. For various additional parameters we refer the reader to Table I. The signals received at all BSs are recorded for offline evaluation.

III. SIGNAL PROCESSING ARCHITECTURE AND EVALUATION CONCEPT

We will now explain, in brief, the general signal processing steps performed in the offline evaluation chain mentioned earlier. For further details we refer the reader to [1].

Synchronization: The carrier frequency of the BS is synchronized by using Global Positioning System (GPS) fed reference normals that have a stability of about 10^{-9}. The mobile terminals estimate their CFO from downlink reference signals and pre-compensate their Uplink transmission accordingly. Compared to the sub-carrier spacing, the remaining offset of less than 200 Hz is small enough to neglect residual inter-carrier interference (ICI).

Channel Estimation: A pilot based approach similar to LTE [36.211] is used for channel estimation. Within each transmit time interval (TTI), the fourth and eleventh (out of 14) OFDM symbol is reserved for pilots. Interference between pilot symbols of different UEs is avoided by a code-orthogonal design. Thus, an estimate $\hat{\mathbf{h}}_{m,k}$ of each link between BS m and UE k is estimated for every second sub-carrier. Time and frequency interpolation are carried out separately to estimate the channel for all other sub-carriers.

Noise Estimation: In the measurement setup only 30 physical resource blocks (PRBs) out of 100 PRBs are used for the transmission of data. Thus, a computation of the received power on the other 70 PRB serves as an estimate for the noise variance $\hat{\sigma}_m^2$ at BS m. The signal power $p_{\text{s},m}$ is determined by computing the difference of the average power per subcarrier, received from both mobile terminals at the 30 PRB used for data transmission and $\hat{\sigma}_m^2$. The SNR_m at BS m is then given by

$$\text{SNR}_m = \frac{p_{\text{s},m}}{\hat{\sigma}_m^2}. \tag{1}$$

Symbol Detection: If residual synchronization errors are neglected, and we assume a flat fading channel on each sub-carrier of bandwidth $\Delta F = 15$ kHz, the received signal of each symbol on a single OFDM sub-carrier at BS m can be stated as

$$\mathbf{y}_m = \mathbf{h}_{m,1}x_1 + \mathbf{h}_{m,2}x_2 + \mathbf{n}_m, \tag{2}$$

where $\mathbf{y}_m \in \mathbb{C}^{[N_{\text{bs}}\times 1]}$ are the signals received by the N_{bs} antennas of BS m, $\mathbf{h}_{m,k} \in \mathbb{C}^{[N_{\text{bs}}\times 1]}$ denotes the channel gain vector from UE k to BS m, $x_k \in \mathbb{C}$ is a symbol transmitted by UE k, and $\mathbf{n}_m \in \mathbb{C}^{[N_{\text{bs}}\times 1]}$ denotes additive, white Gaussian noise with zero mean and covariance $E\{\mathbf{n}_m\mathbf{n}_m^H\} = \sigma_m^2\mathbf{I}$. The transmit power is included in the channel coefficients and we model $E\{x_k x_k^H\} = 1$. Note that maximum number of receive antennas per BS is $N_{\text{bs}} = 2$ in our test system.

The set of BSs that form a cooperation cluster is denoted by $\mathcal{C}$ with elements $\{c_1 \dots c_C\}$, where the cooperation cluster size is denoted by $C = |\mathcal{C}|$. The corresponding transmission model for the cluster is given by

$$\mathbf{y}_\mathcal{C} = \begin{bmatrix} \mathbf{h}_{c_1,1} & \mathbf{h}_{c_1,2} \\ \vdots & \vdots \\ \mathbf{h}_{c_C,1} & \mathbf{h}_{c_C,2} \end{bmatrix} \begin{bmatrix} x_1 \\ x_2 \end{bmatrix} + \begin{bmatrix} \mathbf{n}_{c_1} \\ \vdots \\ \mathbf{n}_{c_C} \end{bmatrix}, \tag{3}$$

where $\mathbf{y}_\mathcal{C} \in \mathbb{C}^{[CN_{\text{bs}}\times 1]}$ are the signals received by the CN_{bs} antennas of the cluster.

The following detection concepts are considered:

- Independent decoding of both UEs by different BSs, using interference rejection combining (IRC) in the case of $N_{\text{bs}} > 1$.

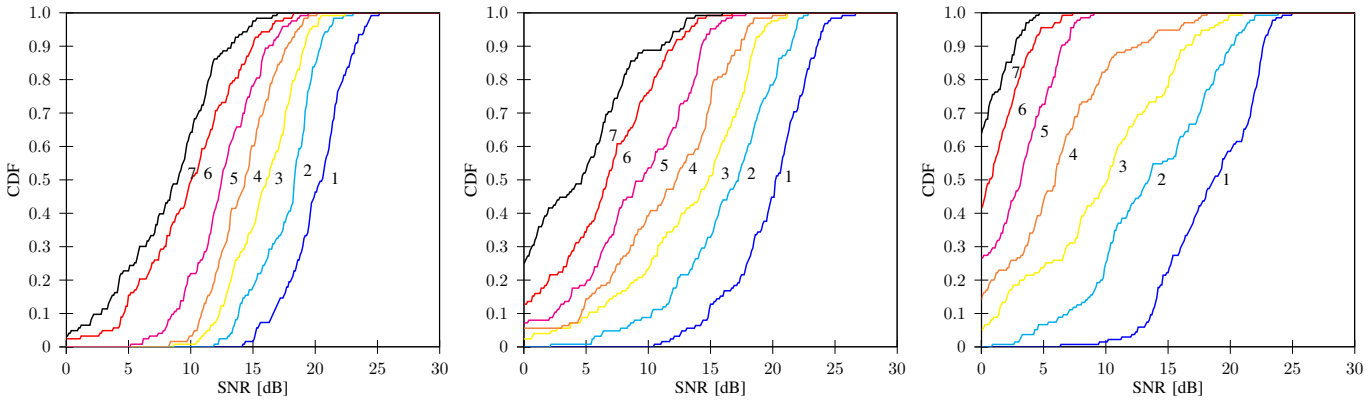

(a) $\Phi_t = 0°$ (b) $\Phi_t = 6°$ (c) $\Phi_t = 12°$

Fig. 2. CDF of SNR at is instantaneously achieved at a certain number of BSs (between one and seven BSs).

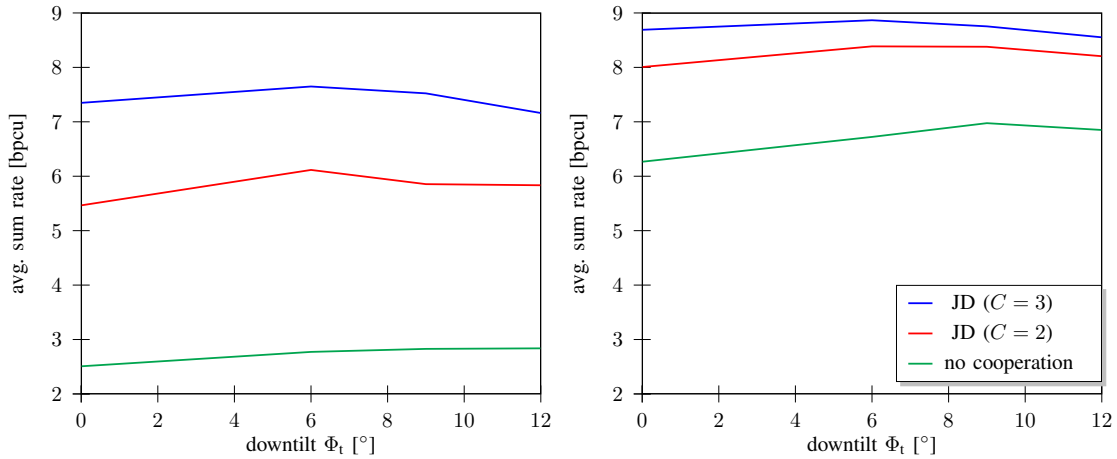

(a) $N_{bs} = 1$ (b) $N_{bs} = 2$

Fig. 3. Avg. rate over downtilt for either one or two BS antennas

- Both UEs are decoded by the same BS, using a linear detector.
- $C - 1$ BSs forward their received signal to another BS, where both UEs are decoded jointly (joint detection (JD)).

Equalization itself is generally based on the same MMSE filters that were described in [9].

Demodulation and Decoding: After equalization, signal-to-interference-plus-noise ratios (SINRs) are estimated via an error vector magnitude approach, followed by soft demodulation. The demodulator output is fed into an LTE Rel. 8 compliant decoding chain that uses codes listed in Table II.

IV. Field Trial Results

The route traversed by the measurement car, traveling at a speed of about 6 km/h, is depicted in Figure 1 (black curve). It passes through surroundings that are representative of an urban area, characterized by broad roads with two lanes in each direction as well as tracks for trams, and sidewalks on either side. Both sides of the road are flanked by large apartments of more than 20 m in height. Thus, there is often a line-of-sight (LOS) between the UEs and one or more BSs and good coverage over the complete route.

During the field trial, the BSs capture an 80 ms block of their received signal every 10 s. At the same time, UEs continuously transmitted codewords (each spanning 1 TTI (1 ms)) continuously, switching cyclically through all 8 MCSs given in Table II — ranging from low code rate 4QAM to high code rate 64QAM. For each loop through all MCSs, the maximum achievable rate is determined — assuming a constant channel for at least the duration of one loop — by emulating a perfect rate adaptation. The achieved rate is obtained by averaging over all loops of one measurement and denoted by $r_{k,p}$ for UE k and position p. For further information on field trial evaluation procedure we refer the reader to [4]. The BSs that are considered for joint decoding of the UEs are determined by a minimum pathloss criterion while UEs, in the non-cooperative case, are decoded at the BS that is able to decode the highest rate codeword.

In summary, the field trial is subject to the following assumptions and limitations:

- Assignment of the same resources to UEs located with fixed distance in close proximity is rather unlikely in a

non-cooperative cellular system with single antenna BSs.

- No rate adaptation and hybrid automatic repeat request (HARQ) due to offline signal processing. The genie rate adaptation scheme (described above) diminishes the diversity gain of JD because each codeword can be decoded at a different BS even in the non-cooperative case.
- No background interference has been considered and, thus, no interference floor is visible.
- Both UEs transmit continuously at maximum power.

In order to study the impact of the BS antenna downtilt, the same route was traversed for different downtilts of $\Phi_\mathrm{t} = 0°, 6°, 9°, 12°$. Figure 1 shows the sum rate ($r_p = r_{1,p} + r_{2,p}$) that was achieved for JD of two BSs with $N_\mathrm{bs} = 2$ BS antennas at each measurement point for each downtilt considered. We see that the sum rate shows rather little fluctuations which is a benefit of JD as shown in a previous publication [10]. Please note that the measurements with different downtilts were conducted one after another. Thus, certain variations in the surroundings and measurement locations were inevitable. However, we will focus on a statistical evaluation in the following for which the accuracy of the results was tested by additional calibration measurements.

Figure 2 shows the cumulative distribution function (CDF) of the SNR that is achieved simultaneously at an increasing numbers of BSs for different downtilts of $0, 6, 12°$. Comparing the case of $\Phi_\mathrm{t} = 0°$ with the case of $\Phi_\mathrm{t} = 6°$, we see that the variance of SNR increases with downtilt because the reception of signals at larger tilts is more focused and, thereby, shows a stronger dependence on the UE location. The results also indicates the potential benefit of JD — using two BSs or more — because a high signal-to-noise ratio (SNR) is instantly achieved at several BSs. Taking the result for a downtilt of 6° as an example, we see that the SNR at three different BSs is above 15 dB in about 50 % of the measurements. This observation is supported by the average sum-rate shown in Figure 3 for JD and non-cooperative detection. The average sum rate for a setup with one receive antenna per BS is shown in Figure 3(a) and the case for two receive antennas in Figure 3(b). In both cases, the downtilt has no significant impact which is remarkable as Figure 2 shows that the average power of the received signal decreases with the downtilt. The major reason for this finding is that the UE rates are mostly limited by inter-user interference rather than by noise. The sum-rate is increasing with downtilt. In the non-cooperative $N_\mathrm{bs} = 1$ case, because of an improved UEs separation: the probability that both UEs are decoded at the same BS is decreases steadily with downtilt from 13 % to 6 %. In the case of $N_\mathrm{bs} = 2$ receive antennas per BS, the UEs signals can be spatially separated at a single BS. As a consequence, detection of both UEs at the same BS achieves much better results.

The user rate CDFs for non-cooperative detection and JD at two BSs are plotted in Figure 4. The curves attest the rate improvements that are achievable using JD and show that

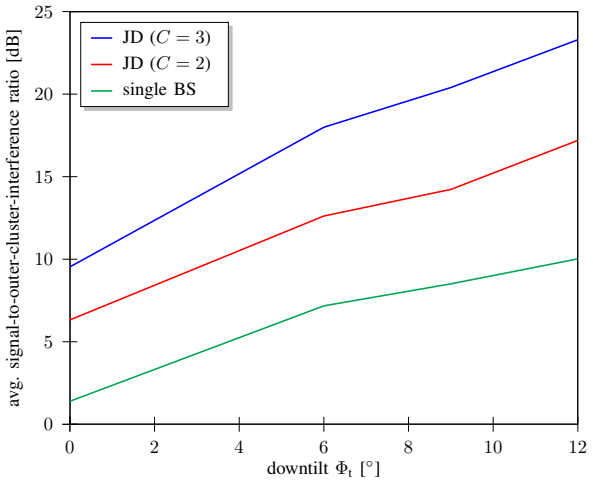

Fig. 5. Average SOCIR using JD of either 2 or 3 BSs

cooperation increases fairness and reduces outage probability. The curves also confirm that downtilt has only a minor impact on the user rate in our field trial system where only intra-cluster interference is considered due to limited number of UEs. For cellular systems, however, outer cluster interference is an important factor, in particular because the size of cooperation clusters is limited due to practical signaling and backhaul constraints. Going back to Figure 2, we see substantial signal propagation to BSs that are outside the interference cluster, where it causes interference. When we compare Figure 2(b) and Figure 2(c), we see that the severity of this interference strongly depends on the downtilt that is applied. In case of 12° downtilt, three BSs have a received signal power of about 10 dB (instead of 15 dB for $\Phi_\mathrm{t} = 6°$) in 50 % of the measurements, but, at the same time, the interference caused at other BSs is substantially reduced. In order to evaluate the trade-offs we compute the SOCIR at each measurement position p which we define as

$$\mathrm{SOCIR}(p) = \frac{\sum\limits_{m \in \mathcal{C}} p_{\mathrm{s},m}}{\sum\limits_{\forall m \setminus m \in \mathcal{C}} p_{\mathrm{s},m}}. \tag{4}$$

Thus, SOCIR is the sum of the received signal power at all BSs outside the cooperation cluster. The average SOCIR for reception at a single BS and cluster sizes of $C = 2$ and $C = 3$ is plotted in Figure 5. In the case of a single BS in the cluster, the received signal at all but one BS is considered as interference. For all cases, the average SOCIR increases with the downtilt showing that the benefit of a potentially larger average signal power for small downtilts is outweighed by the interference caused at BSs outside the cluster and thus downtilt optimization retains its important role in the deployment of cellular systems even when (partial) cooperation between BSs is used.

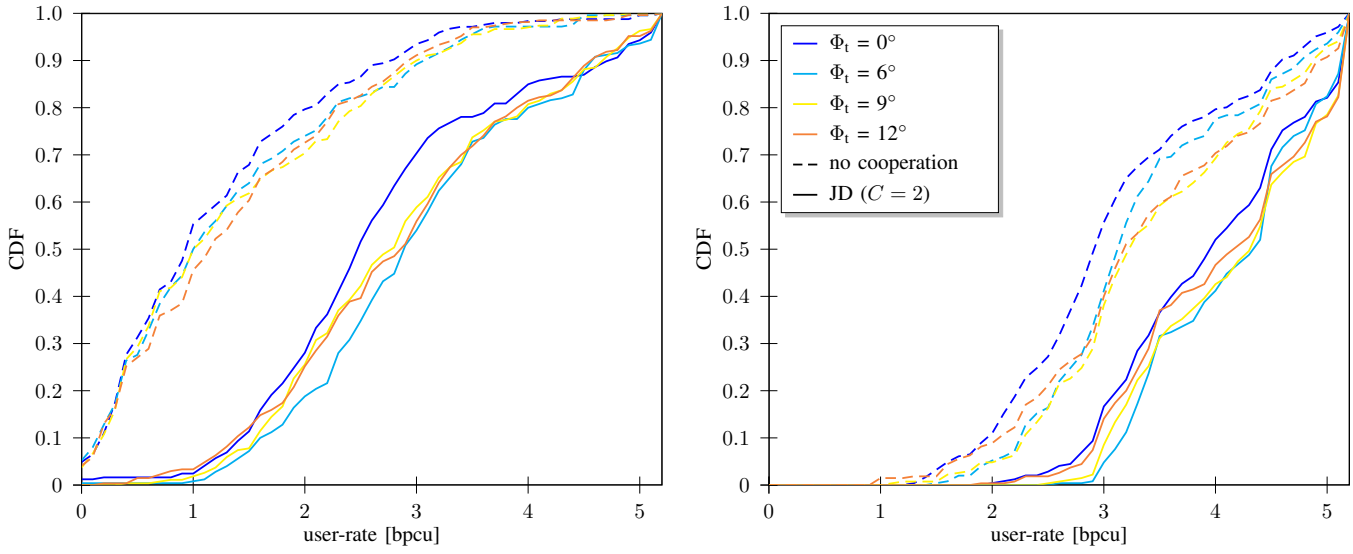

(a) $N_{\text{bs}} = 1$ (b) $N_{\text{bs}} = 2$

Fig. 4. CDF of user rates for non-cooperative and JDof $C = 2$ BSs

V. Conclusions

In this contribution, we presented field trial results for uplink CoMP. Two UEs were moved through an urban cellular testbed with a total of 16 BSs, a setup which allows the assessment of realistic performance gains that are achievable using CoMP. In particular, we investigated the impact of antenna downtilt on the received signal power and data rates. In our evaluation, we did not only considered the received signal at BSs that are part of the cooperation cluster, but also the radiation of power across the cluster border (which is to be avoided because of the interference it causes). We showed that there's a significant impact of different downtilt settings on the SOCIR for a representative urban scenario. At the same time, our study shows that downtilt has a small impact on achievable rates in the CoMP, as long as received power is in a regime, where intra-cluster interference is the limiting factor.

Our results should be compared to system level simulation results, where they could be used for validation of the simulation models in future work. In future field trial campaigns, we will consider additional interferers and the dependence of UE rates on the downtilt.

Acknowledgement

The research leading to these results has received funding from the European Commission's seventh framework programme FP7-ICT-2009 under grant agreement no 247223 also referred to as ARTIST4G. The authors would like to thank the German Ministry for Education and Research (BMBF) for funding the test equipment that is essential for the field trials presented. Further, this work would not have been possible without support from Patrick Marsch, Ainoa Navarro Caldevilla, Sven-Einar Breuer, Vincent Kotzsch, André Zoch, Stefan Boob, and Eckhard Ohlmer.

References

[1] M. Grieger, P. Marsch, Z. Rong, and G. Fettweis, "Field trial results for a coordinated multi-point (CoMP) uplink in cellular systems," in *International ITG Workshop on Smart Antennas*, 2010.

[2] P. Marsch, M. Grieger, and G. Fettweis, "Field trial results on different uplink coordinated Multi-Point (CoMP) concepts in cellular systems," in *IEEE GLOBECOM '10*, 2010.

[3] S. Venkatesan, "Coordinating base stations for greater uplink spectral efficiency: Proportionally fair user rates," in *IEEE PIMRC '07*, 2007.

[4] P. Marsch, M. Grieger, and G. Fettweis, "Large scale field trial results on different uplink coordinated Multi-Point (CoMP) concepts in an urban environment," in *IEEE Wireless Communications and Networking Conference (WCNC '11)*, Cancun, Mexico, 2011.

[5] P. Marsch, A. Fehske, and G. Fettweis, "Increasing mobile rates while minimizing cost per bit — cooperation vs. denser deployment," in *7th International Symposium on Wireless Communication Systems (ISWCS '10)*, 2010.

[6] J. Niemela and J. Lempiainen, "Impact of mechanical antenna downtilt on performance of WCDMA cellular network," in *IEEE Vehicular Technology Conference, VTC 2004-Spring*, 2004.

[7] L. Thiele, T. Wirth, M. Schellmann, Y. Hadisusanto, and V. Jungnickel, "MU-MIMO with localized downlink base station cooperation and downtilted antennas," in *IEEE International Conference on Communications Workshops (ICCW '09)*, 2009.

[8] L. Thiele, T. Wirth, K. Börner, M. Olbrich, V. Jungnickel, J. Rumold, and S. Fritze, "Modeling of 3D field patterns of downtilted antennas and their impact on cellular systems," in *International ITG Workshop on Smart Antennas WSA '09*, Berlin, Germany, 2009.

[9] M. Grieger, P. Marsch, and G. Fettweis, "Large scale field trial results on uplink CoMP with multi antenna base stations," in *IEEE Vehicular Technology Conference, VTC '11-Fall*, San Francisco, USA, 2011.

[10] P. Marsch, M. Grieger, and G. Fettweis, "Large scale field trial results on different uplink coordinated multi-point (CoMP) concepts in an urban environment," in *IEEE Wireless Communications and Networking Conference (WCNC '11)*, 2011.